Stress and Temperature Dependence of the Paramagnetic Resonance Spectrum of Nickel Fluosilicate*†

W. M. WALSH, JR.‡
Gordon McKay Laboratory, Harvard University, Cambridge, Massachusetts
(Received January 19, 1959)

The crystalline field splitting of the ground state spin triplet of divalent nickel in the fluosilicate, $NiSiF_6 \cdot 6\,H_2O$, has been measured at room temperature as a function of hydrostatic pressure to 10 000 kg/cm² and uniaxial stress to 150 kg/cm². The anisotropic compressibility and thermal expansion of this trigonal crystal have also been determined. Combining these data with the known variation of the splitting with temperature, its dependence on isothermal unit cell geometry and on temperature at constant unit cell dimensions is calculated. The splitting is found to be independent of volume within experimental error but proves to be quite sensitive to unit cell shape. The deduced *explicit* temperature dependence is three times larger than that measured at atmospheric pressure. The magnitude and geometrical variation of the crystalline field splitting may be qualitatively understood using a static, ionic model of the $(Ni \cdot 6H_2O)^{2+}$ octahedral complex. A rather general analysis of the explicit temperature dependence indicates, however, that low-frequency lattice vibrations play a dominant role in determining the observed value of the splitting.

The resonance line widths are observed to increase monotonically and quite nonlinearly with increasing pressure. This broadening is discussed in terms of isotropic and anisotropic exchange interactions. In agreement with earlier conclusions of Ollom and Van Vleck it is inferred that the two mechanisms are of comparable importance in this paramagnetic salt.

INTRODUCTION

THE energy level separations of ions in the solid state, which may be studied by absorption spectroscopy, give detailed information concerning the symmetry and strength of the local crystalline potential. Since this potential depends directly on the relative positions of the various electric charges it is a function of the stress to which the crystal is subject and of the lattice temperature.

This has been most clearly demonstrated in the case of nuclear quadrupole resonance experiments performed as a function of hydrostatic pressure and temperature by Kushida, Benedek, and Bloembergen.[1] Using the equation of state of the crystal the quadrupole resonance frequency variations were analyzed to separate the explicit effects of sample geometry and lattice vibrations. These dependences of the crystalline field gradient were then compared with appropriate theoretical models. Shulman, Wyluda, and Anderson[2] have investigated the effect of uniaxial stress on the nuclear magnetic resonance of In^{115} in InSb.

The temperature and hydrostatic pressure dependences of the sharp-line optical absorption spectrum of Eu^{2+} in europium zinc double nitrate single crystals have been studied by Hellwege and Schröck-Veitor.[3] Unfortunately the detailed equation of state of this complex crystal was not known so that the interpretation was limited, though the explicit effect of lattice vibrations as well as sample geometry was noted.

To our knowledge the only previous paramagnetic resonance (PMR) experiment involving other than thermal effects was performed by Van Wieringen[4] who observed the pressure-induced wurzite-to-blende polymorphic transition of ZnS containing Mn^{2+} as an impurity. Changes in the manganese spectrum after successive compressions in a separate press could be seen since this transition is metastable at room temperature.

We have used the PMR technique to study the small crystalline field splitting, D, of the ground state of Ni^{2+} in nickel fluosilicate as a function of hydrostatic pressure to 10 000 kg/cm² and uniaxial stress to 150 kg/cm² at room temperature.[5,6] These are apparently the first electron spin resonance experiments performed under such conditions.[7]

In order to relate the stress and temperature[8,9] dependences of the splitting to the geometry of the lattice the highly anisotropic equation of state was also measured. A thermodynamic analysis indicates how D varies with isothermal unit cell volume and shape and with the temperature explicitly, i.e., at constant average geometry. It is interesting to note that the temperature dependence of crystalline field splittings in paramagnetic salts has been ascribed to

* Supported by a Joint Services contract.
† Based on part of a thesis presented to the Department of Physics, Harvard University, May, 1958 in partial fulfillment of the requirements for the degree of Doctor of Philosophy.
‡ General Electric Company Predoctoral Fellow (1956–1958).
[1] Kushida, Benedek, and Bloembergen, Phys. Rev. **104**, 1099 (1956).
[2] Shulman, Wyluda, and Anderson, Phys. Rev. **107**, 953 (1957).
[3] K. H. Hellwege and W. Schröck-Vietor, Z. Physik **143**, 451 (1955).
[4] J. S. Van Wieringen, Physica **19**, 397 (1953).
[5] W. M. Walsh, Jr., and N. Bloembergen, Phys. Rev. **107**, 904 (1957).
[6] W. M. Walsh, Jr., Bull. Am. Phys. Soc. Ser. II, **3**, 178 (1958).
[7] The hydrostatic pressure dependence of the PMR spectra of two dilute chromium salts is reported in the following paper.
[8] R. P. Penrose and K. W. H. Stevens, Proc. Phys. Soc. (London) **A63**, 29 (1950).
[9] J. W. Meyer, thesis, University of Wisconsin, 1955 (unpublished).

thermal expansion alone[10] whereas in nuclear quadrupole resonance only the explicit temperature dependence was considered until pressure experiments were used to distinguish between the two mechanisma.

A qualitative understanding of the magnitude of the fluosilicate splitting and of its isothermal geometrical dependence is obtained using a static, ionic model of the $(Ni\cdot 6H_2O)^{2+}$ complex. However, a crude analysis of the strong explicit temperature dependence of D in terms of low-frequency lattice vibrations cannot, apparently, be reconciled with the static model.

Line width measurements as a function of hydrostatic pressure show an increase of over 100% while interionic distances decrease by less than 2%. This effect is attributed to increasing exchange interactions between neighboring ions via intervening atomic orbitals and is discussed in terms of isotropic and anisotropic exchange mechanisms which have previously been proposed for this salt.[11,12]

I. THE CRYSTALLINE FIELD AND THE SPIN HAMILTONIAN

The crystal structure of nickel fluosilicate, $NiSiF_6\cdot 6H_2O$, is inferred from that of the isomorph, nickel chlorostannate, $NiSnCl_6\cdot 6H_2O$, which has been investigated in detail by Pauling.[13] There is one molecule per unit cell, the crystal being made up of $(Ni\cdot 6H_2O)^{2+}$ $(SnCl_6)^{2-}$ complexes arranged on a slightly distorted bcc lattice. The deformation corresponds to a compression along a body diagonal whence the symmetry is trigonal or rhombohedral. The individual complexes form apparently regular octahedra with the metallic ions as centers. The Ni-Ni distance in the fluosilicate is 6.27A and the rhombohedral angle is 96°5′.[14]

It is evident that the Ni^{2+} ion is exposed to a predominantly cubic electric field with a weaker trigonal component superposed. The free ion, having eight $3d$ electrons, is in a ^3F ground state. The spin, $S=1$, may be considered to arise from two holes in the $3d$ shell whose spins are aligned. The octahedral cubic electric field due to the water molecules leaves an orbital singlet several thousands of wave numbers below two orbital triplets.[15] The ground state remains triply spin degenerate in a purely cubic electric field as has recently been experimentally verified by Low.[16] The trigonal crystalline field component and the spin-orbit interaction split the spin triplet into a doublet and a singlet,[15] the doublet being lowest in the fluosilicate.[17] The behavior of this ground spin triplet in a magnetic field may be described by the spin Hamiltonian[18]

$$\mathcal{H}=\beta[g_{\parallel}H_zS_z+g_{\perp}(H_xS_x+H_yS_y)]+D(S_z^2-\tfrac{2}{3}). \quad (1)$$

The $\hat{z}$ axis is the trigonal axis of the crystal, the orthogonal $\hat{x}$ and $\hat{y}$ axes being taken arbitrarily in the plane perpendicular to the symmetry axis.

Previous PMR investigations of this salt[8,9,19] show $g_{\parallel}\simeq g_{\perp}\simeq 2.30$ and $D=-0.52$ cm^{-1} at room temperature. The splitting, D, decreases nonlinearly in magnitude with decreasing temperature to a constant value of -0.12 cm^{-1} below 20°K. It is this strongly temperature-dependent splitting which makes nickel fluosilicate attractive for our purposes.

II. THE SPLITTING AND THE EQUATION OF STATE

In principle both the deviation of the g-value from that of the free electron, $\Delta g\equiv g-2.0023$, and the crystalline field splitting, D, should be treated as functions of the stress and temperature state of the crystal. Since, however, Δg does not prove to be a sensitive parameter in these experiments it will be sufficient to focus our attention on D. The detailed relation between the splitting of the spin energy levels and the local crystalline field will be considered in Sec. V. At present it is only necessary to note that the crystalline potential involves the position coordinates of the contributing charges. These coordinates are functions of time due to thermal vibrations whence the observed value of D is a time average, $\langle D\rangle_t$ which depends not only on the average value of the source coordinates (purely geometrical dependence) but also on the detailed character of the vibrations (explicit temperature dependence).

The latter point may be easily seen if we consider the particular case of an ionic lattice subject to purely harmonic vibrations. Each ion's contribution to the various symmetry components of the electric potential depends on various powers of the ion's position coordinates with respect to the point of observation. If, for example, a distance is harmonically modulated, i.e., $d(t)=d_0(1+\epsilon\cos\omega t)$, the time average value of d^n is $\langle d^n\rangle_t=d_0{}^n[1+n(n\mp 1)\epsilon^2/4]$, $n\gtrless 0$. This does, in general, affect the average value of the crystalline potential, yet the average geometry of the lattice is not changed.

Formally we should treat D as a function of all those coordinates, $X_i(i=1,\cdots,8$ for the fluosilicate structure assuming water molecules may be considered to be rigid bodies), required to specify the average geometry of the unit cell and of the normal modes, $\xi_j(j=1,\cdots,3N-3$ where N is the number of atoms in the crystal), required to specify the thermal vibrations of the ions about their average positions. The X_i and ξ_j are all functions of temperature and of the stress applied to the crystal.

[10] Bagguley, Bleaney, Griffiths, Penrose, and Plumpton, Proc. Phys. Soc. (London) **61**, 551 (1948).
[11] J. F. Ollom and J. H. Van Vleck, Physica **17**, 205 (1951).
[12] Ishiguro, Kambe, and Usui, Physica **17**, 310 (1951).
[13] L. Pauling, Z. Krist. **72**, 482 (1930).
[14] R. W. G. Wyckoff, *Crystal Structures* (Interscience Publishers, Inc., New York, 1951), Vol. III.
[15] H. A. Bethe, Ann. Physik **3**, 133 (1929); *Splitting of Terms in Crystals* (Consultants Bureau, New York, 1958).
[16] W. Low. Phys. Rev. **109**, 247 (1958).
[17] J. Becquerel and W. Opechowski, Physica **6**, 1039 (1939).
[18] B. Bleaney and K. W. H. Stevens, Repts. Progr. in Phys. **16**, 108 (1953).
[19] Holden, Kittel, and Yager, Phys. Rev. **75**, 1443 (1949).

Unfortunately only the external dimensions of the unit cell could be specified experimentally. Thus D will be regarded as a function of the unit cell volume $X_1 \equiv V = Gl_{\|}l_{\perp}^2$, the unit cell "shape," $X_2 \equiv \sigma = G' l_{\|}/l_{\perp}$, and the temperature, T. The symbols, $l_{\|}$ and $l_{\perp}$, refer to the crystal lengths parallel and perpendicular to the trigonal axis, respectively; G and G' are geometrical scaling factors which will be eliminated through the use of logarithmic derivatives.

In order to evaluate $(\partial D/\partial \ln V)_{\sigma,T}$, $(\partial D/\partial \ln\sigma)_{V,T}$, and $(\partial D/\partial T)_{V,\sigma}$ three independent PMR experiments must be performed. We have measured D as a function of (1) temperature at constant (atmospheric) pressure (this merely confirms the earlier measurements), (2) hydrostatic pressure, P, at constant (room) temperature, and (3) uniaxial compressive stress, U, directed along the symmetry axis at constant (room) temperature. The relationships between the measured and desired quantities are

$$\left(\frac{\partial D}{\partial T}\right)_P = \left(\frac{\partial D}{\partial \ln V}\right)_{\sigma,T}\left(\frac{\partial \ln V}{\partial T}\right)_P + \left(\frac{\partial D}{\partial \ln\sigma}\right)_{V,T}\left(\frac{\partial \ln\sigma}{\partial T}\right)_P + \left(\frac{\partial D}{\partial T}\right)_{V,\sigma}, \quad (2)$$

$$\left(\frac{\partial D}{\partial P}\right)_T = \left(\frac{\partial D}{\partial \ln V}\right)_{\sigma,T}\left(\frac{\partial \ln V}{\partial P}\right)_T + \left(\frac{\partial D}{\partial \ln\sigma}\right)_{V,T}\left(\frac{\partial \ln\sigma}{\partial P}\right)_T, \quad (3)$$

$$\left(\frac{\partial D}{\partial U}\right)_T = \left(\frac{\partial D}{\partial \ln V}\right)_{\sigma,T}\left(\frac{\partial \ln V}{\partial U}\right)_T + \left(\frac{\partial D}{\partial \ln\sigma}\right)_{V,T}\left(\frac{\partial \ln\sigma}{\partial U}\right)_T. \quad (4)$$

It is evident that the derivatives $(\partial \ln V/\partial T)_P$, etc., are required to complete the evaluation of the theoretically interesting quantities $(\partial D/\partial \ln V)_{\sigma,T}$, etc. This corresponds to measuring the equation of state of the crystal for the stress and temperature range covered in the PMR experiments.

It should be noted that Eqs. (2)–(4) mask the basic complexity of D in that only the observed variables are used: $D=D(V,\sigma,T)$, whereas $D=D(V,\sigma,X_3\cdots X_8, \xi_1\cdots\xi_{3N-3})$ from the analytical point of view. Thus the derivatives of D with respect to volume, shape and temperature obtainable from equations (2)–(4) really involve the undertermined, internal coordinates of the unit cell as well as the normal modes of vibration:

$$\left(\frac{\partial D}{\partial T}\right)_{V,\sigma} = \sum_{i=3}^{8}\frac{\partial D}{\partial X_i}\left(\frac{\partial X_i}{\partial T}\right)_{V,\sigma} + \sum_{j=1}^{3N-3}\frac{\partial D}{\partial \xi_j}\left(\frac{\partial \xi_j}{\partial T}\right)_{V,\sigma}, \quad (5)$$

$$\left(\frac{\partial D}{\partial V}\right)_{\sigma,T} = \frac{\partial D}{\partial V} + \sum_{i=3}^{8}\frac{\partial D}{\partial X_i}\left(\frac{\partial X_i}{\partial V}\right)_{\sigma,T} + \sum_{j=1}^{3N-3}\frac{\partial D}{\partial \xi_j}\left(\frac{\partial \xi_j}{\partial V}\right)_{\sigma,T}, \quad (6)$$

$$\left(\frac{\partial D}{\partial \sigma}\right)_{V,T} = \frac{\partial D}{\partial \sigma} + \sum_{i=3}^{8}\frac{\partial D}{\partial X_i}\left(\frac{\partial X_i}{\partial \sigma}\right)_{V,T} + \sum_{j=1}^{3N-3}\frac{\partial D}{\partial \xi_j}\left(\frac{\partial \xi_j}{\partial \sigma}\right)_{V,T}. \quad (7)$$

Unbracketed partial derivatives imply that all the other independent variables are fixed.

III. EXPERIMENTAL TECHNIQUES

The PMR spectrometer is indicated in Fig. 1. Audio-frequency modulation of the magnetic field and phase-sensitive detection were used, i.e., dX''/dH *versus* H was recorded. Sensitivity on narrow lines was $\sim 10^{15}\Delta H$ spins for unity signal-to-noise ratio at room temperature. An *AFC* circuit locked the 2K25 klystron to the sample cavity frequency. This frequency (8500–9500 Mc/sec) was measured using a cavity wavemeter calibrated against a frequency marker system. The current-stabilized magnet was rotatable for alignment with sample axes and the field was measured using a Pound-Watkins nuclear resonance spectrometer and a mineral oil sample.

The microwave coupling into the BeCu high pressure bomb and the coaxial cavity have been described and illustrated in a preliminary communication.[5] Hydrostatic pressures up to 10 000 kg/cm^2 were generated and measured by standard techniques.[20]

Uniaxial compressive stress was applied parallel to the symmetry axis of single crystal samples with the arrangement shown in Fig. 2. Lead weights drove a

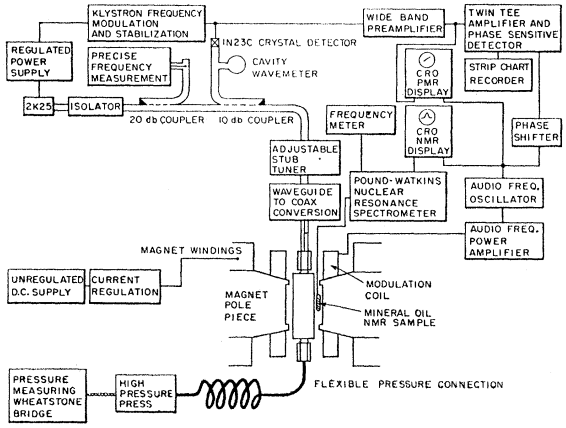

FIG. 1. Block diagram of paramagnetic resonance spectrometer.

[20] P. W. Bridgman, *The Physics of High Pressure* (G. Bell and Sons, London, 1952).

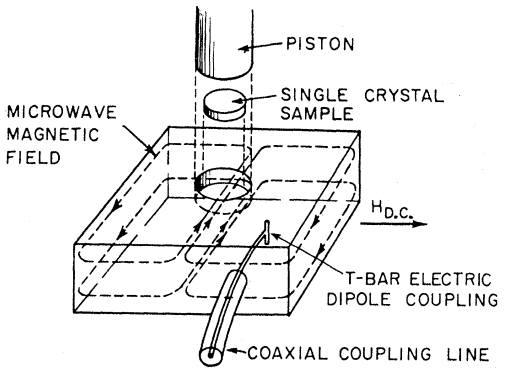

FIG. 2. Apparatus for the uniaxial stress experiment.

0.25-in. diameter Dural piston into a TE_{102} mode rectangular brass cavity. The crystal was placed in a cylindrical hole milled in the polystyrene cavity filler piece. Microwave coupling via a coaxial cable with an electric dipole termination was used. The cavity and piston assembly was supported in the magnet by a brass stand. Initially we planned to drive the piston with the pressure generating press but this proved unnecessary since the samples cracked with a loading greater than $\sim$150 kg/cm^2 so that only 20 kg of lead weights were required to cover the useable range of stress.

As indicated in the previous section, the resonance experiments may be interpreted only if the crystal dimensions are determined under the same experimental conditions as is the crystalline field splitting. In principle a complete x-ray investigation of the sample as a function of stress and temperature would give the required information about the internal $(X_3 \cdots X_8)$ as well as the external (V,σ) coordinates and even some data on the lattice vibration spectrum. As a practical compromise Type SR-4 A-7, Baldwin-Lima-Hamilton Corporation resistance strain gauges were used to measure percentage changes of external crystal dimensions. Two gauges, $R_{\parallel}$ and $R_{\perp}$, were cemented parallel and perpendicular, respectively, to the trigonal axis of a single crystal fluosilicate sample. A third control gauge, R_c, was placed near the sample but was not bonded to it. The requisite electrical leads were brought through a multiterminal high pressure plug to a switching box and Wheatstone bridge. To determine linear compressibilities the plug was inserted in a high pressure bomb and the variations of $(R_{\parallel}-R_c)$, $(R_{\perp}-R_c)$, and $(R_{\parallel}-R_{\perp})$ were measured as a function of applied pressure. The corresponding sample dimension changes were easily computed using the gauge factor, $G \equiv (\delta R/R)/(\delta l/l)$, provided with the gauges. To measure thermal dependences the sample and plug assembly was placed in a brass can which in turn was placed in a temperature-regulated water bath covering the 0° to 50°C range. Several attempts to measure the deformation of the crystal subject to uniaxial compression gave inconsistent, unreproducible results. It was finally decided to estimate this part of the equation of state on the basis of the linear hydrostatic compressibilities as will be discussed in the next section.

The accuracy of this strain gauge technique is rather poor due to the unknown perfection of the gauge-to-crystal bond. Using Duco cement the fluosilicate measurements are reproducible to within 5%. It is important to cure the bonds at 100°C or higher for several days in order to remove all possible solvent from the cement; otherwise hysteresis is observed upon cycling pressure or temperature. It is probably wisest to consider the measured dimension changes as lower limits since bond slippage is certainly the major source of error.

Large single crystals of nickel fluosilicate may easily be grown from water solution by slow evaporation. However, crystals grown at room temperature usually contain pockets of the mother liquor and show a "shell" structure indicative of periodic variations in the rate of deposition on the seed probably due to temperature fluctuations. Unsuccessful attempts were made to grow better samples at a higher, regulated temperature ($\sim$45°C) while slowly moving the seed crystal in the mother liquor. Homogeneous, unstrained crystals were finally obtained by evaporation of the solution in a refrigerator at $\sim$5°C using material obtained from the City Chemical Corporation, New York City.

For the hydrostatic pressure PMR experiments fluosilicate crystals were prepared in the form of tori (0.25 in. O.D.$\times$0.10 in. I.D.$\times$0.10 in. thickness) by dissolving away the unwanted material. The trigonal axis lay in the plane of the torus. The uniaxial stress samples had to be carefully prepared as homogeneous strain was desired. Disks (0.20 in. O.D.$\times$0.07 in. thickness) with the trigonal axis perpendicular to the plane of the disk were initially shaped by the dissolution technique and the final few thousandths of an inch were removed on a milling machine using a very sharp tool. To ensure homogeneous deformation care was

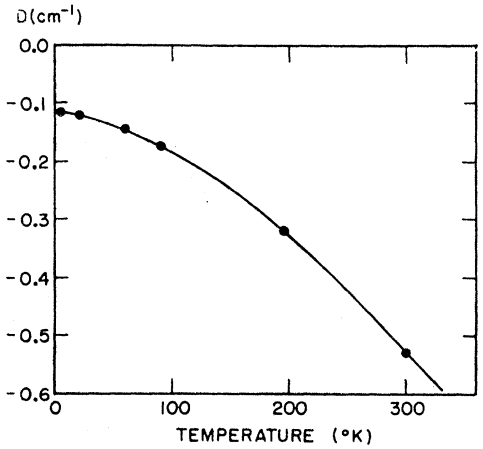

FIG. 3. Temperature dependence of the crystalline field splitting at atmospheric pressure.

taken to have the faces of the disks parallel and the sides accurately perpendicular to the faces. These samples were coated with silicone grease before inserting in the microwave cavity in order to permit free radial expansion as the uniaxial loading increased. Despite these precautions compressive stresses greater than 150 kg/cm^2 invariably resulted in fracture of the samples.

IV. EXPERIMENTAL RESULTS

A. Paramagnetic Resonance

The temperature dependence of D measured by Penrose and Stevens[8] and Meyer[9] is shown in Fig. 3. We have checked the slope of this curve near room temperature and find $(\partial D/\partial T)_P = -19.5\times10^{-4}$ cm^{-1}/°C in good agreement with the earlier results.

The hydrostatic pressure experiments were performed with the applied field along the trigonal axis of the crystal. In this case the eigenvalues of the spin-Hamiltonian, Eq. (1), diverge linearly and may be accurately labeled by $S_z=1$, 0 and -1: $W_{\pm1}=D/3 \pm g\beta H$, $W_0=-2D/3$. Two allowed magnetic dipole transitions ($\Delta S_z=\pm1$), observed at constant frequency, occur at $H_1=-(D+h\nu)/g\beta$ and $H_2=(h\nu-D)/g\beta$ for $D<-h\nu$ as is the case at room temperature and pressure. This situation is illustrated in Fig. 4.

When pressure is applied the resonance lines move about in magnetic field as schematically indicated in Fig. 5, where both the line centers and *peak derivative points* are shown. The actual data are complicated by a shift of the microwave cavity frequency to lower frequencies as pressure is increased due to increased dielectric filling of the cavity. This shift amounts to 800 Mc over a range of 10 000 kg/cm^2 when a Teflon cavity filler piece is used.[5] In Fig. 5 the data have been corrected to a constant frequency of 9000 Mc for clarity.

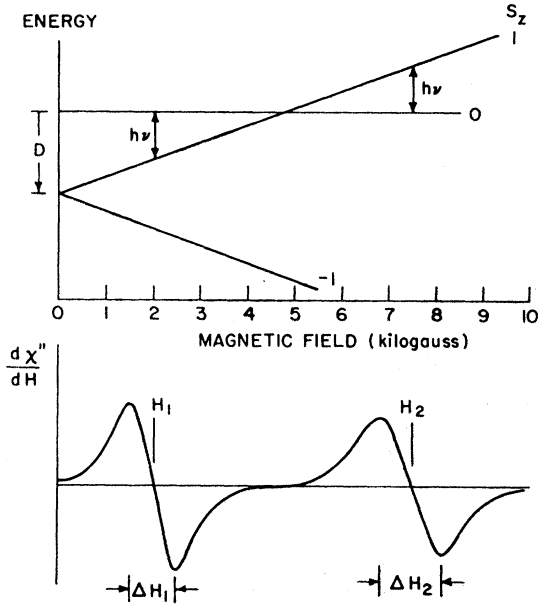

FIG. 4. Energy level diagram and derivative of the absorption spectrum of Ni^{2+} in the fluosilicate when the field is applied parallel to the trigonal axis and $D<-h\nu$.

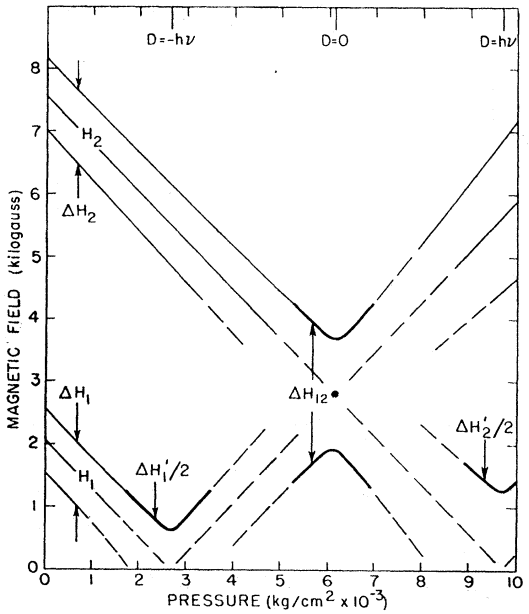

FIG. 5. Pressure dependence of line centers and peak derivative points corrected to constant microwave frequency ($\nu=9000$ Mc/sec). Broken lines indicate regions of excessive overlap of the two resonances.

The strong pressure dependence of the crystalline field splitting, D, is shown in Fig. 6. Since D varies over a range of more than $2h\nu$ and the absorption lines are 1000 gauss or more from peak to peak it is necessary to compute D in different ways at different pressures. Below 1000 kg/cm^2 the two transitions $(1\rightarrow0)$, centered at H_1, and $(0\rightarrow1)$, centered at H_2, are clearly resolved whence D and g may both be calculated. When the magnitude of the splitting becomes approximately equal to the microwave quantum, as occurs for pressures around 2650 kg/cm^2, only the higher field

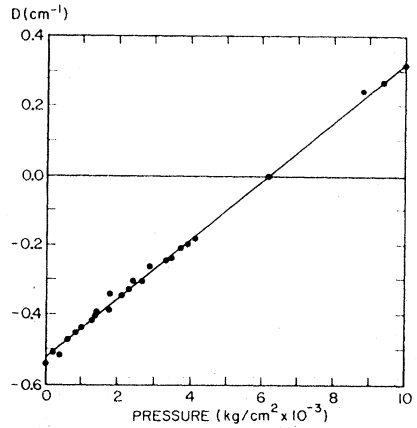

FIG. 6. Pressure dependence of the crystalline field splitting.

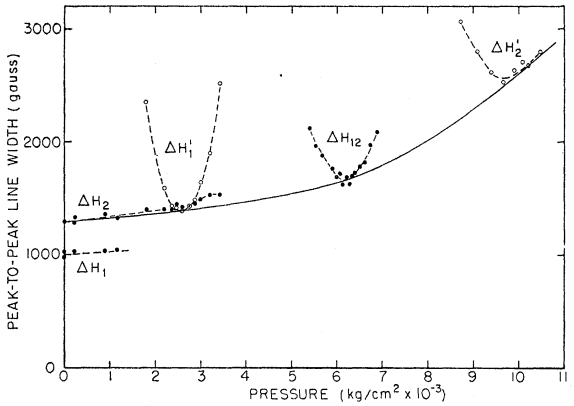

FIG. 7. Pressure dependence of peak-to-peak line widths.

transition, centered at H_2, is unambiguously defined. The low field line, H_1, which corresponds to the transition $(1\rightarrow 0)$ at lower pressures now becomes mixed with the $(-1\rightarrow 0)$ transition. Thus when $D=-h\nu$ we see one resonance line centered at zero field which has twice the intensity of the high field resonance. For higher pressure, i.e., $D>-h\nu$, the low field line again becomes ill defined as the $(1\rightarrow 0)$ transition is suppressed and the $(-1\rightarrow 0)$ transition moves to higher field values. Since g does not vary appreciably with presssure the average value 2.30[21] is used to calculate D from the values of H_2 in this pressure range where $D\sim -h\nu$. A check is provided when $D=-h\nu$ as then the apparent half-width, $\Delta H_1'/2$, of the double intensity, zero field line, H_1, passes through a minimum indicating that the two transitions $(1\rightarrow 0)$ and $(-1\rightarrow 0)$ are exactly superposed. As the pressure is raised above 2650 kg/cm² the high field line, H_2, continues to move to lower field values whereas the low field line, H_1, which is now the $(-1\rightarrow 0)$ transition, moves to higher fields. Near 4000 kg/cm² the two resonance lines overlap to such an extent that no data may be taken. Near 6200 kg/cm² one composite line is observed whose width, ΔH_{12}, passes through a minimum corresponding to exact superposition of the $(0\rightarrow 1)$ and $(-1\rightarrow 0)$ transitions, i.e., $D=0$. At still higher pressures the two lines separate again, H_1 moving to higher fields and H_2 to lower fields. Since the lines now have almost twice their original widths it is only as $D\rightarrow h\nu$ near 9750 kg/cm² that H_1 becomes sufficiently resolved to permit calculation of D, assuming g to be constant as before. Again a consistency check is provided when $D=h\nu$ as then the half-width, $\Delta H_2'/2$, of the low field resonance H_2 [now of double intensity since the $(0\rightarrow 1)$ and $(0\rightarrow -1)$ transitions are superposed at zero field] passes through a minimum. The resultant plot of D *versus* pressure, Fig. 6, shows that these various determinations are consistent. The slope of the straight line is $(\partial D/\partial P)_T=0.834\times 10^{-4}$ cm^{-1}/kg/cm².

The various line width data (peak-to-peak derivative) are plotted in Fig. 7. Only the *minima* of $\Delta H_1'$, ΔH_{12}, and $\Delta H_2'$ are meaningful as is evident from Fig. 5 and the preceding description. The solid curve drawn in Fig. 7 is considered to adequately represent the available data save for the initial values of ΔH_1 which are about 20% less than the values of ΔH_2 in this range. The minimum in $\Delta H_1'$, however, agrees very well with ΔH_2 at the same pressure.

The uniaxial compression data were taken with the magnetic field applied perpendicular to the crystal's symmetry axis due to practical geometrical considerations. In this orientation the eigenvalues of the spin Hamiltonian are not linear functions of H but are given by $W_{\pm 1}=-D/6\pm[D^2/4+(g\beta H)^2]^{\frac{1}{2}}$, $W_0=D/3$. Only one transition is observable with $h\nu\sim 0.3$ cm^{-1} at room temperature: $H_3=h\nu(1-D/h\nu)^{\frac{1}{2}}/g\beta$. Since the cavity frequency changes by only 3 Mc/sec out of 9247 Mc/sec in the course of this experiment the variation of H_3 directly measures the stress dependence of D. Figure 8 shows the dependence of H_3 on sample loading, U, (mass/sample face area). The resultant slope of D *versus* U is $(\partial D/\partial U)_T=-1.66\times 10^{-4}$ cm^{-1}/kg/cm².

Each point of Fig. 8 is the average of five slow magnetic field sweeps through the line in both directions. The resultant line center is defined to within 10 gauss despite the peak-to-peak line width of 840 gauss in this orientation. It is necessary to monitor the temperature carefully in the course of this experiment as $(\partial H_3/\partial T)_P \simeq 14$ gauss/°C, which is quite appreciable when the total shift is only 60 gauss and data are taken over several hours.

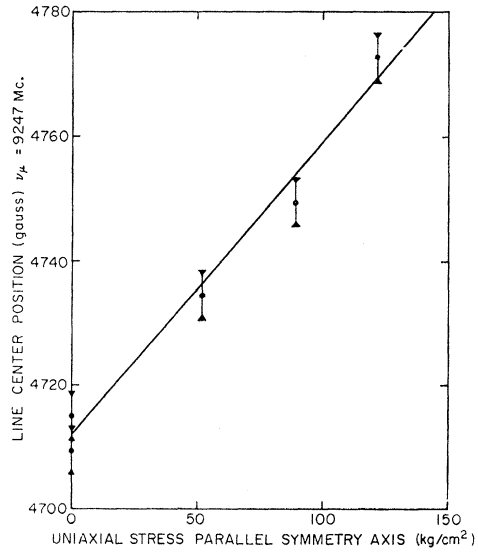

FIG. 8. Uniaxial compressive stress dependence of the resonance line center with the magnetic field perpendicular to the trigonal axis.

[21] In an earlier communication[5] a constant g-value of 2.34±0.02 was quoted. Additional data indicate that $g=2.30\pm 0.04$ is a more trustworthy value. The pressure dependence of D is essentially unchanged by this small revision of g.

TABLE I. Results of paramagnetic resonance and strain measurements.

At $T=25°C$ and $P=1$ kg/cm² $D=-0.52$ cm^{-1} and $g=2.30$	
Observed	Deduced
(a) Temperature dependence (0–25°C)	
$\left(\frac{\partial \ln l_{\parallel}}{\partial T}\right)_P = 0.50\times10^{-4}$ (°C)$^{-1}$	$\left(\frac{\partial \ln V}{\partial T}\right)_P = 0.31\times10^{-4}$ (°C)$^{-1}$
$\left(\frac{\partial \ln l_{\perp}}{\partial T}\right)_P = -0.095\times10^{-4}$ (°C)$^{-1}$	$\left(\frac{\partial \ln \sigma}{\partial T}\right)_P = 0.60\times10^{-4}$ (°C)$^{-1}$
$\left(\frac{\partial D}{\partial T}\right) = -19.5\times10^{-4}$ cm^{-1}/°C	
(b) Hydrostatic pressure dependence ($T=25°C$)	
$\left(\frac{\partial \ln l_{\parallel}}{\partial P}\right)_T = -0.90\times10^{-6}$ (kg/cm²)$^{-1}$	$\left(\frac{\partial \ln V}{\partial P}\right)_T = -5.3\times10^{-6}$ (kg/cm²)$^{-1}$
$\left(\frac{\partial \ln l_{\perp}}{\partial P}\right)_T = -2.2\times10^{-6}$ (kg/cm²)$^{-1}$	$\left(\frac{\partial \ln \sigma}{\partial P}\right)_T = 1.3\times10^{-6}$ (kg/cm²)$^{-1}$
$\left(\frac{\partial D}{\partial P}\right)_T = 0.834\times10^{-4}$ cm^{-1}/(kg/cm²)	
(c) Uniaxial stress dependence ($T=25°C$)	
$\left(\frac{\partial \ln l_{\parallel}}{\partial U}\right)_T = -2.0\times10^{-6}$ (kg/cm²)$^{-1}$ [a]	$\left(\frac{\partial \ln V}{\partial U}\right)_T = -0.90\times10^{-6}$ (kg/cm²)$^{-1}$
$\left(\frac{\partial \ln l_{\perp}}{\partial U}\right)_T = 0.55\times10^{-6}$ (kg/cn²)$^{-1}$ [a]	$\left(\frac{\partial \ln \sigma}{\partial U}\right)_T = -2.5\times10^{-6}$ (kg/cm²)$^{-1}$
$\left(\frac{\partial D}{\partial U}\right) = -1.66\times10^{-4}$ cm^{-1}/(kg/cm²)	
(d) Explicit dependences on temperature, volume, and shape evaluated at $T=25°C$, $P=1$ kg/cm²	$\left(\frac{\partial D}{\partial T}\right)_{V,\sigma} = -(58\pm5)\times10^{-4}$ cm^{-1}/°C
	$\left(\frac{\partial \ln D}{\partial \ln V}\right)_{\sigma,T} = -0.3\pm2$
	$\left(\frac{\partial \ln D}{\partial \ln \sigma}\right)_{V,T} = -125\pm10$

[a] Estimated values

It is believed that the strain produced in this experiment was truly elastic as the value of D measured upon removal of the maximum stress agreed with the initially unstrained value within the experimental error. The degree of homogeneity may be only crudely inferred from the absence of any measurable line-broadening in the course of the experiment. Fracture of samples for $U>150$ kg/cm² is clear evidence that the strain must be inhomogeneous though the low shear strength of this material implies that the degree of inhomogeneity may be quite small even at fracture.

B. Linear Strain Measurements

Using the strain gauge technique described in Sec. III it is relatively easy to measure linear strains parallel and perpendicular to the trigonal axis as a function of hydrostatic pressure or temperature changes. Thermal strain data were taken in the range 0° to 50°C at atmospheric pressure. Hydrostatic compressibilities were measured from 1 to 1500 kg/cm² at room temperature. The numerical results are given in Table I. A high degree of anisotropy is found, particularly in the thermal distortion of the crystal: upon heating it

expands along the trigonal axis and *contracts* perpendicular to it.

As mentioned earlier we were unable to obtain trustworthy experimental values for the strains produced by uniaxial compression. In order to proceed with the thermodynamic analysis of the PMR data an "educated guess" was based on elasticity considerations. Using the condensed notation $1=xx$, $2=yy$, $3=zz$, $4=yz$, $5=zx$, and $6=xy$, the elastic constant matrix for a trigonal crystal without a plane of reflection symmetry perpendicular to the threefold (z) axis is given by[22]

$$s_{ij}=\begin{vmatrix} s_{11} & s_{12} & s_{13} & s_{14} & -s_{25} & 0 \\ s_{12} & s_{11} & s_{13} & -s_{14} & s_{25} & 0 \\ s_{13} & s_{13} & s_{33} & 0 & 0 & 0 \\ s_{14} & -s_{14} & 0 & s_{44} & 0 & s_{25} \\ -s_{25} & s_{25} & 0 & 0 & s_{44} & s_{14} \\ 0 & 0 & 0 & s_{25} & s_{14} & \frac{1}{2}(s_{11}-s_{12}) \end{vmatrix}. \quad (8)$$

When hydrostatic pressure, P, is applied, the stress components are $X_1=X_2=X_3=-P$, $X_4=X_5=X_6=0$. The resultant nonvanishing strains are $x_1=x_2=-(s_{11}+s_{12}+s_{13})P$ and $x_3=-(s_{33}+2s_{13})P$. Normalizing to unit pressure we have

$$\left(\frac{\partial \ln l_{\parallel}}{\partial P}\right)_T=-(s_{33}+2s_{13}), \quad (9)$$

$$\left(\frac{\partial \ln l_{\perp}}{\partial P}\right)_T=-(s_{11}+s_{12}+s_{13}). \quad (10)$$

When uniaxial compressive stress, U, is applied along the trigonal axis $X_3=-U$, $X_1=X_2=X_4=X_5=X_6=0$, assuming the sample is free to expand in the xy plane. The strains are $x_1=x_2=-s_{13}U$ and $x_3=-s_{33}U$ or

$$\left(\frac{\partial \ln l_{\parallel}}{\partial U}\right)_T=-s_{33}, \quad (11)$$

$$\left(\frac{\partial \ln l_{\perp}}{\partial U}\right)_T=-s_{13}. \quad (12)$$

Experimentally we have evaluated (9) and (10): $(s_{33}+2s_{13})=0.90\times10^{-6}(\text{kg/cm}^2)^{-1}$ and $(s_{11}+s_{12}+s_{13})=2.2\times10^{-6}(\text{kg/cm}^2)^{-1}$. These are insufficient to determine s_{13} and s_{33} but allow reasonable estimates to be made: $s_{13}\simeq-0.55\times10^{-6}(\text{kg/cm}^2)^{-1}$ and $s_{33}\simeq2.0\times10^{-6}$ (kg/cm^2).

The various deduced values of the geometrical and explicit temperature derivatives of the crystalline field splitting based on Eqs. (2), (3), and (4) are given in Table I. Of the two geometrical parameters the unit cell shape is by far the most important: $(\partial \ln D/\partial \ln\sigma)_{V,T}=-125\pm10$, whereas the volume dependence is zero within experimental error: $(\partial \ln D/\partial \ln V)_{\sigma,T}=-0.3\pm2$. The most striking conclusion is that D depends even more strongly on temperature after geometrical corrections are made: $(\partial D/\partial T)_{V,\sigma}=-(58\pm5)\times10^{-4}$ cm^{-1}/°C as opposed to $(\partial D/\partial T)_P=-19.5\times10^{-4}$ cm^{-1}/°C. The factor of 3 difference is due to the shape-dependent contribution to the variation of D caused by temperature change at constant pressure. It is $\frac{2}{3}$ as large as the explicit temperature dependence and of opposite sign.

V. DISCUSSION OF RESULTS

A. Isothermal Geometrical Effects

As indicated in Eqs. (6) and (7), the measured derivatives of D with respect to volume and shape of the unit cell, $(\partial D/\partial V)_{\sigma,T}$ and $(\partial D/\partial\sigma)_{V,T}$, depend not only on V and σ but also on the internal degrees of freedom and the geometrical dependence of the lattice vibrations. Though the latter point is not *a priori* negligible (the strong explicit temperature dependence of D would, in fact, lead to the opposite conclusion) it must be ignored due to insufficient data.[23]

The six internal coordinates, $X_3\cdots X_8$, are the "volumes" and "shapes" of the $(\text{Ni}\cdot6\text{H}_2\text{O})^{2+}$ and $(\text{SiF}_6)^{2-}$ octahedra and their azimuthal orientations relative to the unit rhombohedron. For simplicity an idealized, ionic model of the $(\text{Ni}\cdot6\text{H}_2\text{O})^{2+}$ complex alone will be used as a basis for discussing the experimental results.

The positions of the six water molecules relative to the Ni^{2+} ion may be defined by the radial distance, d, and the polar angle, α, made by the radius vectors with the trigonal axis as sketched in Fig. 9. The electrostatic potential, $\Phi(\mathbf{r})$, seen by the nickel ions is considered to be produced by the electric dipole moments, μ_i, of these water molecules. Assuming that the d-orbitals of the ion do not overlap with the nearest-neighbor oxygen atoms the potential,

$$\Phi(\mathbf{r})=\sum_{i=1}^{6}\frac{\mu(\mathbf{r}-\mathbf{d}_i)\cdot\mathbf{d}_i/d_i}{|\mathbf{r}-\mathbf{d}_i|^3}, \quad (13)$$

may be expanded in spherical harmonics, $Y_n{}^m(\theta,\phi)$. Only terms with $n=2$ or 4 need be retained when operating on d orbitals[18] and only terms with $m=0,\pm3$ are allowed due to the threefold rotational symmetry of the structure. The reduced expansion is usually written in the form

$$\Phi'(\mathbf{r})=Q[(10)^{\frac{1}{2}}(Y_4{}^3-Y_4{}^{-3})-(7)^{\frac{1}{2}}Y_4{}^0]+aY_2{}^0+bY_4{}^0, \quad (14)$$

where the terms in a and b drop out in purely cubic symmetry.

The perturbation of the ^3F ground state of Ni^{2+} by the potential (14) plus the spin-orbit interaction,

[22] W. A. Wooster, *A Textbook on Crystal Physics* (Cambridge University Press, Cambridge, 1938).

[23] In principle, at least, measurements of D as a function of geometry over a wide range of temperature would permit evaluation of such a dependence (see reference 1 for examples).

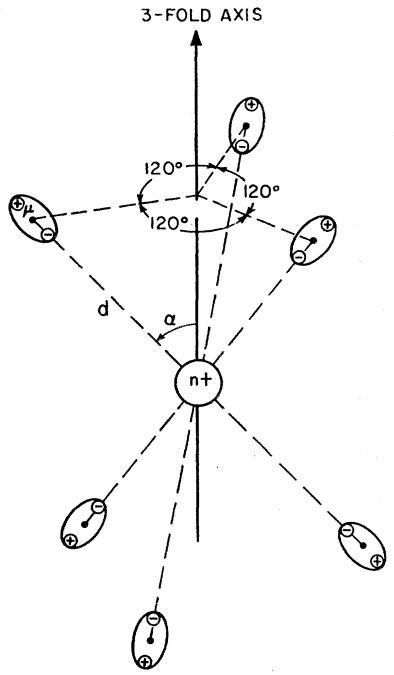

FIG. 9. Idealized model of an ion surrounded by six electric dipoles forming an octahedron "stretched" along the trigonal axis ($\alpha<54°\,44'$).

$\lambda\mathbf{L}\cdot\mathbf{S}$, has been treated in detail by Becquerel and Opechowski[17] and extended by Penrose and Stevens.[8] It is assumed that the cubic crystalline field is the dominant perturbation, i.e., $Q\gg a,b,\lambda$. In the process of evaluating matrix elements the parameters Q, a, and b are averaged over the radial part, $f(r)$, of the $3d$ wave function and new parameters $\bar{Q}$, $\bar{a}$, and $\bar{b}$ are defined:

$$\bar{Q}=-\frac{e}{14}\left(\frac{7}{\pi}\right)^{\frac{1}{2}}\frac{\langle r^4\rangle_{\mathrm{Av}}}{r^4}Q, \tag{15a}$$

$$\bar{a}=-\frac{e}{14(5\pi)^{\frac{1}{2}}}\frac{\langle r^2\rangle_{\mathrm{Av}}}{r^2}a, \tag{15b}$$

$$\bar{b}=-\frac{e}{14(\pi)^{\frac{1}{2}}}\frac{\langle r^4\rangle_{\mathrm{Av}}}{r^4}b, \tag{15c}$$

where $\langle r^n\rangle_{\mathrm{Av}}\equiv\langle f|r^n|f\rangle$. Evaluating these parameters for the potential due to the six water dipoles arranged as shown in Fig. 9 we find

$$\bar{Q}=\frac{5}{2\sqrt{2}}e\mu\frac{\langle r^4\rangle_{\mathrm{Av}}}{d^6}\sin^3\alpha\cos\alpha, \tag{16a}$$

$$\bar{a}=-\frac{9}{35}e\mu\frac{\langle r^2\rangle_{\mathrm{Av}}}{d^4}(1-3\cos^2\alpha), \tag{16b}$$

$$\bar{b}=\frac{5}{28}e\mu\frac{\langle r^4\rangle_{\mathrm{Av}}}{d^6}(35\cos^4\alpha-30\cos^2\alpha+3+7\sqrt{2}\sin^3\alpha\cos\alpha). \tag{16c}$$

Since the trigonal distortion of the water octahedron is small it is convenient to expand these expressions to first order in $(\alpha-\alpha_0)$ where $\alpha_0=54°\,44'$ is the polar angle for the regular configuration

$$\bar{Q}\simeq\frac{5}{9}e\mu\frac{\langle r^4\rangle_{\mathrm{Av}}}{d^6}\left[1+\frac{(\alpha-\alpha_0)}{\sqrt{2}}\right], \tag{17a}$$

$$\bar{a}\simeq-\frac{18\sqrt{2}}{35}e\mu\frac{\langle r^2\rangle_{\mathrm{Av}}}{d^4}(\alpha-\alpha_0), \tag{17b}$$

$$\bar{b}\simeq\frac{15\sqrt{2}}{14}e\mu\frac{\langle r^4\rangle_{\mathrm{Av}}}{d^6}(\alpha-\alpha_0). \tag{17c}$$

The expressions for the spin-Hamiltonian parameters taken to first order in $\bar{a}$ and $\bar{b}$ from the papers of Becquerel and Opechowski[17] and Penrose and Stevens[8] are

$$g_{\parallel}=g_0\left[1-\frac{4\lambda}{15\bar{Q}}\left(1-\frac{3\bar{a}-\bar{b}}{9\bar{Q}}\right)\right], \tag{18}$$

$$g_{\perp}=g_0\left[1-\frac{4\lambda}{15\bar{Q}}\left(1+\frac{\bar{a}-2\bar{b}}{6\bar{Q}}\right)\right], \tag{19}$$

$$D=\frac{4\lambda^2}{45\bar{Q}^2}(\tfrac{3}{2}\bar{a}+\tfrac{2}{3}\bar{b}). \tag{20}$$

Due to lack of resolution we were unable to measure the anisotropic part of the deviation of the g-tensor from the free electron value, $g_0=2.0023$, but may at least specify the isotropic part:

$$\Delta g\equiv g-g_0=-\frac{4\lambda g_0}{15\bar{Q}}=0.30. \tag{21}$$

The free-ion value of the spin-orbit coupling constant for Ni^{2+} is $\lambda=335$ cm^{-1} [24] which implies $\bar{Q}\sim600$ cm^{-1}. However, direct optical measurements of the cubic field splittings of Ni^{2+} in MgO[16] and other data[18] indicate that λ is closer to -250 cm^{-1} in ionic crystals.[25] The cubic electric field parameter, $\bar{Q}$, is, therefore, likely to be ~430 cm^{-1}.

To calculate $\bar{Q}$, $\bar{a}$, and $\bar{b}$ numerical values of $\langle r^2\rangle_{\mathrm{Av}}$ and $\langle r^4\rangle_{\mathrm{Av}}$ are required. Using the Hartree-Fock radial $3d$ wave function computed for Cu^+ by Hartree and Hartree[26] these numbers have been estimated to be

$$\langle r^2\rangle_{\mathrm{Av}}\simeq0.36\times10^{-16}\text{ cm}^2,$$
$$\langle r^4\rangle_{\mathrm{Av}}\simeq0.38\times10^{-32}\text{ cm}^4.$$

Since the ionic radius of Cu^+ is 0.97 A and that of Ni^{2+} is only 0.70 A these values of $\langle r^2\rangle_{\mathrm{Av}}$ and $\langle r^4\rangle_{\mathrm{Av}}$ are too

[24] O. Laporte, Z. Physik **47**, 761 (1928).
[25] The cubic field parameter Dg used by Low[16] and others is $3\bar{Q}/2$ in our notation which is that of Becquerel and Opechowski.[17]
[26] D. R. Hartree and W. Hartree, Proc. Roy. Soc. (London) **A157**, 490 (1936).

large, as is the ratio $\langle r^4\rangle_{Av}/\langle r^2\rangle_{Av}$. The numerical value of the water molecule electric dipole moment is found to be

$$\mu=4.0\times10^{-18}\text{ esu},$$

by a calculation similar to that described by Polder[27] in connection with the energy levels of Cu^{2+} in $CuSO_4\cdot5H_2O$. Using these values of $\langle r^4\rangle_{Av}$ and μ and taking $\alpha=\alpha_0$ and $d=2$ A[14] Eq. (17a) yields

$$\bar{Q}=320\text{ cm}^{-1}.$$

The 30% discrepancy between our estimate and the probable experimental value does not seem unreasonable since we have neglected the contributions to $\bar{Q}$ from the rest of the lattice. We have also ignored the possible effects of lattice vibrations on $\bar{Q}$ as Δg does not appear to be appreciably temperature dependent.[8]

Combining Eqs. (17), (20), and (21) the expression for the crystalline field splitting may be written

$$D=\frac{5\sqrt{2}}{16}e\mu(\Delta g)^2\left(\frac{5}{7}\frac{\langle r^4\rangle_{Av}}{d^6}-\frac{27}{35}\frac{\langle r^2\rangle_{Av}}{d^4}\right)(\alpha-\alpha_0). \quad (22)$$

Substituting the appropriate numerical values Eq. (22) yields

$$D=-50.4(\alpha-\alpha_0)\text{ cm}^{-1}.$$

The room temperature value, $D=-0.52$ cm^{-1}, implies $(\alpha-\alpha_0)=0.6°$ which is considerably less than the deviation from cubic symmetry to be expected if the polar angle, α, characteristic of the water octahedron, were to be identical with the polar angle, β, made by a rhombohedral axis with the trigonal axis. The rhombohedral angle of nickel fluosilicate is $\Gamma\simeq96°$, which leads to $\beta\simeq59°$ or $(\beta-\alpha_0)\simeq4°$. It is, however, probable that the water octahedron is indeed more regular than is the over-all unit cell.[13] It is even possible that the water octahedron is exactly regular and that the trigonal component of the crystalline field results entirely from the distorted cube of $(SiF_6)^{2-}$ groups which are the next-nearest neighbors of the nickel ion. Unfortunately the calculation becomes very unwieldy if the model is extended to include the entire unit cell. It should also be noted that lattice vibrations do affect D strongly so that the static model cannot be expected to give more than the correct order of magnitude at best.

Despite the apparent limitations it is interesting to estimate the sensitivity of the splitting to volume and shape changes of the simple octahedral model. The volume dependence is not precisely determined since $\bar{a}$ and $\bar{b}$ both contribute significantly to D, yet vary as d^{-4} and d^{-6}, respectively. (The term in $\bar{b}$ is usually neglected in calculations of this sort[17,28,29] for a variety of reasons which do not appear to be valid.) Since, however, $\bar{a}\simeq-4\bar{b}$ Eqs. (17) and (20) imply that

$$\left(\frac{\partial\ln D}{\partial\ln D}\right)_{\sigma,T}\lesssim\frac{8}{3}.$$

The observed value, $(\partial\ln D/\partial\ln V)_{\sigma,T}=-0.3\pm2$, is not excessively inconsistent with $+8/3$ if we consider that the water octahedron may be less compressible than the unit cell whose deformation is observed.

It might at first appear surprising that the magnitude of D should be expected to increase as volume increases since this weakens the trigonal electric field component. However, the cubic field strength, $\bar{Q}$, also decreases, thus making the electronic charge cloud more polarizable. It is the latter effect which should dominate.

The shape parameter, σ, may be expressed in terms of the polar angle, α, normalized to unity for $\alpha=\alpha_0$ and expanded to first order in $(\alpha-\alpha_0)$:

$$\sigma\simeq1-\frac{3}{\sqrt{2}}(\alpha-\alpha_0). \quad (23)$$

Combining Eqs. (22) and (23) the logarithmic shape derivative may be written

$$\frac{d\ln D}{d\ln\sigma}=\frac{\sigma}{\sigma-1}. \quad (24)$$

Volume is not conserved as α alone is varied but, since the volume dependence of the splitting is weak, the distinction between $d\ln D/d\ln\sigma$ and $(\partial\ln D/\partial\ln\sigma)_{V,T}$ may be ignored. Experimentally we found $(\partial\ln D/\partial\ln\sigma)_{V,T}=-125\pm10$ which implies $(\alpha-\alpha_0)=0.2°$ using Eqs. (23) and (24). This appears to be in reasonable agreement with the value $(\alpha-\alpha_0)=0.6°$ inferred from the magnitude of D. Unfortunately the agreement is probably illusory as we measure external shape changes of the unit cell whereas our model deals only with internal changes which are not likely to be as large since $(\alpha-\alpha_0)$ is evidently much smaller than $(\beta-\beta_0)$. It is now quite clear that experiments of this type are difficult to interpret quantitatively unless the crystal structure is sufficiently simple that measurements of compressibility, etc., specify the positions of *all* atoms in the unit cell as a function of the experimental environment.

B. The Explicit Temperature Dependence

One of the more interesting experimental conclusions is that the temperature dependence of the crystalline field splitting is not solely due to thermally induced changes of the average unit cell geometry. The measured explicit temperature dependence, $(\partial D/\partial T)_{V,\sigma}$, as shown in Eq. (5), arises from vibrations of the sources of the crystalline field and, perhaps, to changes in the average internal geometry of the unit cell which we must ignore due to lack of relevant information.

[27] D. Polder, Physica **9**, 709 (1942).
[28] L. J. F. Broer, Physica **9**, 547 (1942).
[29] P. R. Weiss, Phys. Rev. **73**, 470 (1948).

The ionic model of the $(Ni\cdot 6H_2O)^{2+}$ octahedron could be extended to include dynamic effects by calculating the normal modes of the system as has been done by Van Vleck in treating the Jahn-Teller problem[30] and spin-lattice relaxation.[31] A somewhat less detailed approach has been used in analyzing the temperature variations of nuclear quadrupole resonance frequencies.[32,33,1] It essentially consists in expanding the time dependence of the variable of interest in terms of the (usually unknown) normal modes of vibration of lattice, $\xi_i=\xi_i^0\cos 2\pi\nu_i t$. Thus the crystalline field splitting is written as

$$D(t)=D_0(1+\sum_i A_i\xi_i+\sum_{ij} B_{ij}\xi_i\xi_j+\cdots). \quad (25)$$

The parameter, D_0, is the splitting in the absence of *all* vibrations, i.e., D_0 is the splitting predicted by a truly static model. The coupling constants, A_i and B_{ij}, as well as the ξ_i^0 and ν_i depend on sample geometry in principle. If it may be assumed that the important vibration frequencies, ν_i, are greater than the observation frequency, $\nu_{\text{obs}}\sim 10^{10}$ cps, then the observed value of D will be a simple time average of (25):

$$D_{\text{obs}}\simeq D_0\left(1+\sum_i \frac{B_{ii}\xi_i^{02}}{2}\right). \quad (26)$$

The assumption, $\nu_i\gg\nu_{\text{obs}}$, appears to be reasonable as the line width of the undiluted nickel fluosilicate is not markedly temperature-dependent[34] and the most important modes are likely to be vibrations within the $(Ni\cdot 6H_2O)^{2+}$ groups. Experimental data on such complexes in solution indicate characteristic frequencies $\nu_i\sim 10^{13}$ cps.[35]

The lattice temperature is explicitly introduced by equating the energy of a normal mode to that of a Planck oscillator of the same frequency:

$$2(\pi\xi_i{}^0\nu_i)^2=h\nu_i\left(\tfrac{1}{2}+\frac{1}{e^{h\nu_i/kT}-1}\right), \quad (27)$$

which leads to

$$D=D_0\left[1+\frac{h}{4\pi^2}\sum_i\frac{B_{ii}}{\nu_i}\left(\tfrac{1}{2}+\frac{1}{e^{h\nu_i/kT}-1}\right)\right]. \quad (28)$$

This dependence on T qualitatively resembles that shown in Fig. 3. These data were taken at atmospheric pressure, however, and include not only the explicit temperature effect but also the temperature-dependent geometrical effects. The distinction is an important one in this case as $(\partial D/\partial T)_{V,\sigma}\simeq 3(\partial D/\partial T)_P$.

Since the D *versus* T at constant pressure curve is fairly linear near room temperature, (28) may be approximated on the assumption that $h\nu_i<kT$ or $\nu_i<10^{13}$ cps at room temperature:

$$\tfrac{1}{2}+\frac{1}{e^x-1}\simeq\frac{1}{x}, \quad x<1. \quad (29)$$

Equation (28), taken only to the linear term in T, becomes

$$D\simeq D_0(1+BT), \quad (30)$$

where

$$B\equiv\frac{k}{4\pi^2}\sum_i\frac{B_{ii}}{\nu_i{}^2}. \quad (31)$$

To evaluate B we use the logarithmic derivative

$$\left(\frac{\partial\ln D}{\partial T}\right)_{V,\sigma}\simeq\frac{B}{1+BT}. \quad (32)$$

The experimental value $(\partial\ln D/\partial T)=(112\pm 10)\times 10^{-4}$ $(°C)^{-1}$ implies $B\simeq -47\times 10^{-4}$ $(°C)^{-1}$, $D_0\simeq 1.2$ cm^{-1}.

The positive sign of D_0 is most surprising as the static model predicted $D_0<0$ for the "squashed" cubic configuration which is known to exist in the fluosilicate. Equation (30) implies that D is observed to be negative only because the lattice vibration contribution to D is opposite in sign and larger in magnitude than the static geometrical contribution.

In view of this dilemma a closer examination of the temperature law (28) is desirable. The method has been successfully used to explain the relatively weak temperature dependences observed in nuclear quadrupole resonance. It is usually found that the coupling constants, B_{ii}, which have the dimensions (mass $\times$distance$^2)^{-1}$, may be directly related to the inverse of the moments of inertia of a few torsional vibration modes involving atoms neighboring the observed nuclei.[1] We may analogously consider the moment of inertia, I, of a water molecule performing a torsional oscillation relative to the Ni^{2+} ion:

$$I=M_{H_2O}d^2\simeq 1.2\times 10^{-38}\text{ gm cm}^2.$$

While the infrared experiments indicate vibration frequencies $\nu_i\sim 10^{13}$ cps in solution the linear behavior of D *versus* T at room temperature implies $\nu<10^{13}$ cps. If n modes of frequency $\nu_i\sim 10^{12}$ cps are effective and $B_{ii}=I^{-1}$ then Eq. (31) yields $B\sim 3\times 10^{-4}n$ whereas the experimental number is $\sim 5\times 10^{-3}$. The required number of modes, $n\sim 16$, is not unreasonable since there are twelve degrees of torsional freedom available within the octahedron.

The relatively low vibration frequency also brings to mind the characteristic relaxation time, τ, of water molecules in the liquid ($\tau\sim 10^{-11}$ sec).[36] The extreme

[30] J. H. Van Vleck, J. Chem. Phys. **7**, 72 (1939).
[31] J. H. Van Vleck, Phys. Rev. **57**, 426 (1940).
[32] H. Bayer, Z. Physik **130**, 227 (1951).
[33] T. Kushida, J. Sci. Hiroshima University, **A19**, 327 (1955).
[34] Preliminary experiments indicate anomalously large, temperature dependent line widths in the dilute (Ni,Zn) fluosilicate, however, so that the possibility of lower frequency vibrations ($\nu_i\sim\nu_{\text{obs}}$) cannot be ruled out.
[35] R. Lafont, Compt. rend. **244**, 1481 (1957).
[36] Collie, Hasted, and Ritson, Proc. Phys. Soc. (London) **60**, 145 (1948).

dielectric loss of hydrated crystals at microwave frequencies may indicate that "reorientation" of water molecules also occurs to some extent in the solid state. However, we were unable to find any evidence for motional narrowing[37] of the proton nuclear magnetic resonance in nickel fluosilicate at room temperature.

Another possible mode of effective, low-frequency vibrations might be hindered rotation of the $(Ni\cdot 6H_2O)^{2+}$ complex as a whole within the unit rhombohedron. Such a highly correlated motion seems unlikely but might be potent as the relative orientations of the cubic crystalline field components due to the octahedron and the rhombohedron would be modulated. In general a superposition of two or more cubic fields gives rise to a cubic and an axial component lying along the axis of relative rotation. In the trigonal fluosilicate the net axial field due to this mechanism would be along the trigonal axis.

Many other conjectures as to the origin of the strong explicit temperature dependence of D may be made but a mechanism particular to this specific salt appears to be required in that the rapid variation is not a general property of hydrated, paramagnetic crystals.[38] It seems likely that x-ray analysis of the highly anisotropic thermal expansion would provide a starting point for such a detailed study.

C. Line Width Variation

The rapid, nonlinear increase of the peak-to-peak line width, ΔH, with hydrostatic pressure is shown in Fig. 7. Since magnetic dipole-dipole broadening depends on interspin distance to the inverse third power a linear increase of ΔH of about 5% to 10 000 kg/cm^2 would be expected due to volume reduction. It is not surprising, however, that this mechanism proves inadequate as previous investigations have shown exchange interactions to outweigh the dipolar mechanism in this salt.

While analyzing the low temperature magnetic susceptibility and specific heat measurements of Benzie and Cook,[39] Ollom and Van Vleck[11] were led to suggest that both isotropic and anisotropic or pseudo-dipolar exchange mechanisms[40,41] are present. The magnetic specific heat is attributed to (1) magnetic dipole interactions which may be computed knowing the interspin distance and the g-value; (2) the crystalline field splitting determined from PMR measurements; (3) isotropic exchange which may be determined from the susceptibility and magneto-optical rotation data[42]; and (4) anistropic exchange. When the first three contributions are evaluated as indicated above and subtracted from the total magnetic specific heat the residual contribution, presumably due to anisotropic exchange, is found to be comparable to that due to isotropic exchange. Though this relative magnitude is quite implausible from the theoretical viewpoint[40] it is qualitatively confirmed by the following considerations.

Ishiguro, Kambe, and Usui[12] and Ollom[43] have approximately analyzed the second moments of the resonance curves published by Holden, Kittel, and Yager,[19] assuming only isotropic exchange and normal magnetic dipole interactions to be effective. The deduced values of the exchange constant are roughly 50% larger than those calculated from the susceptibility and magneto-optical rotation experiments. If the anisotropic exchange mechanism were to be included, this descrepancy should be considerably reduced.

Our line width *versus* pressure data also indicate that isotropic exchange cannot be the dominant source of line width. If this were the case we should observe pronounced exchange narrowing[44] at 6200 kg/cm^2 where the splitting goes to zero since exchange would then occur between equivalent nickel spins. A careful search in this pressure region revealed no line width as narrow as those observed at lower pressures. This is compatible with the presence of comparable amounts of isotropic and anisotropic exchange since as D goes to zero the isotropic mechanism will tend to narrow the lines whereas the broadening due to anisotropic exchange will be enhanced as the precession frequencies of all spins become equal.[44] The monotonic pressure dependence of ΔH implies that neither of these effects clearly dominates, which agrees with the original conclusions of Ollom and Van Vleck.

The very nonlinear character of the pressure dependence is reasonable in that both exchange interactions may be expected to vary almost exponentially with interionic distance. Since the nickel ions are well separated in the fluosilicate lattice the exchange path must involve intervening orbitals.[45] This appears to be consistent with the reduced spin-orbit coupling parameter of Ni^{2+} in the solid state which results if the magnetic electrons spend an appreciable part of the time on the nominally diamagnetic ions due to partially covalent bonding.[46,47]

CONCLUSIONS

By combining the results of paramagnetic resonance and crystal strain measurements as a function of hydrostatic pressure, uniaxial stress and temperature, it has been possible to determine the geometrical and explicit thermal dependences of the crystalline field splitting in nickel fluosilicate. There is some ambiguity in the interpretation due to the possibility of non-

[37] Bloembergen, Purcell, and Pound, Phys. Rev. **73**, 679 (1948).
[38] K. D. Bowers and J. Owen, Repts. Progr. in Phys. **18**, 304 (1955).
[39] R. J. Benzie and A. W. Cooke, Proc. Phys. Soc. (London) **A63**, 213 (1950).
[40] J. H. Van Vleck, Phys. Rev. **52**, 1178 (1937).
[41] One could also consider dipole-quadrupole and quadrupole-qudrupole interactions as Ni^{2+} has $S=1$.
[42] J. Becquerel and J. Van den Handel, Physica **6**, 1034 (1939).
[43] J. F. Ollom, thesis, Harvard University, 1952 (unpublished).
[44] J. H. Van Vleck, Phys. Rev. **74**, 1168 (1948).
[45] P. W. Anderson, Phys. Rev. **79**, 350 (1950).
[46] K. W. H. Stevens, Proc. Roy. Soc. (London) **A219**, 542 (1953).
[47] J. Owen, Proc. Roy. Soc. **A227**, 183 (1955).

homogeneous deformation within the unit cell which cannot be measured by the strain gauge technique. While the analysis based on a rigid ionic model of the $(Ni\cdot 6H_2O)^{2+}$ complex gives rough agreement between the magnitude and isothermal geometrical dependence of the splitting this static model should not be taken too seriously since the explicit temperature dependence indicates that the splitting is primarily determined by thermal vibrations. The magnitude of the explicit temperature dependence is consistent with torsional vibrations of the nearest-neighbor water molecules at a frequency close to 10^{12} cps. Since the elastic and thermal properties of this material are markedly anisotropic a more detailed analysis based on a dynamic model of the entire unit cell appears to be required if the splitting variations are to be understood in detail.

The monotonic, nonlinear variation of the PMR line widths with hydrostatic pressure provides qualitative evidence for the presence of appreciable indirect exchange coupling between the nickel spins in the fluosilicate. It appears that both isotropic and anisotropic exchange mechanisms make comparable contributions to the line widths. Though theoretically implausible this is consistent with earlier conclusions drawn from a variety of experimental data.

ACKNOWLEDGMENTS

The author wishes to thank Professor N. Bloembergen who originally suggested this investigation and whose continuing interest and advice have greatly aided in its completion. Professor G. B. Benedek gave freely of his knowledge of high pressure techniques. Dr. J. W. Meyer provided some of the initial samples used and S. Shapiro helped in the preparation of subsequent samples. Dr. S. Foner suggested the use of strain gauges. The invaluable aid of J. Keith, G. Boodry, and J. J. MacDonald in preparing and maintaining the equipment is gratefully acknowledged.

PHYSICAL REVIEW VOLUME 114, NUMBER 6 JUNE 15, 1959

Pressure Dependence of the Paramagnetic Resonance Spectra of Two Dilute Chromium Salts*†

WALTER M. WALSH, JR.‡§
Gordon McKay Laboratory, Harvard University, Cambridge, Massachusetts

(Received January 19, 1959)

The pressure dependences of the spin-Hamiltonian parameters of trivalent chromium in ammonium aluminum alum and potassium cobalticyanide have been measured up to 10 000 kg/cm² near room temperature. In the case of the alum, runs have been made at 0, 24 and 50°C. The g-value remains unchanged while the crystalline field splitting, δ, increases by $\sim 30\%$, $(\partial\delta/\partial P)_T$ decreasing with rising temperature and pressure.

Using an empirically determined equation of state the crystalline field splitting variations are converted to isothermal volume and explicit temperature dependences. These are discussed in terms of static and dynamic crystalline fields but are not satisfactorily explained. This failure is attributed to inhomogeneous internal deformation of the unit cell as a function of stress and temperature.

A room temperature run on the covalent chromicyanide shows the g-value as well as the principal splitting parameter, D, to be nonmonotonic functions of pressure. The rhombic splitting parameter, E, increases quadratically with pressure. Since no attempt was made to determine the crystalline equation of state the resonance data are only qualitatively discussed. It is difficult to reconcile the results with the equivalent crystalline field model of the chromicyanide complex.

I. INTRODUCTION

IN order to distinguish between geometrical and explicit thermal contributions to the average crystalline electric field seen by paramagnetic ions it is necessary to measure the spin-Hamiltonian parameters over an appreciable range of stress and temperature. These results must then be combined with the equation of state of the particular crystal. In the preceding paper we have reported the results of such an analysis of the crystalline field splitting of the paramagnetic resonance (PMR) spectrum of divalent nickel in the concentrated fluosilicate. Due to the trigonal symmetry of that crystal it was necessary to determine the effect of both volume and shape changes of the unit cell. In an effort to reduce the complexity of the problem we have examined the PMR spectrum of trivalent chromium in the cubic crystal, ammonium chromium alum diluted with diamagnetic ammonium aluminum alum, as a function of hydrostatic pressure and temperature.

In both the fluosilicate and the alum the magnetic ion is considered to form a primarily ionic complex with the six nearest-neighbor water molecules. It was, therefore, thought to be of interest to examine the covalent complex $[Cr(CN)_6]^{3-}$ in potassium chromicyanide diluted with diamagnetic potassium cobalticyanide.

* Supported by a Joint Services contract.

† Based on part of a thesis presented to the Department of Physics, Harvard University, May, 1958, in partial fulfillment of the requirements for the degree of Doctor of Philosophy.

‡ General Electric Company Predoctoral Fellow (1956–1958).

§ *Note added in proof.*—In the original abstract of this paper [Phys. Rev. Letters 2, 519 (1959)] the thermal expansion coefficient of ammonium aluminum alum was reported to be negative. This anomalous result is incorrect. The author is indebted to Dr. G. Burns of the IBM Research Center for bringing this error to his attention and for providing a reference to the thermal expansion of several alums.